Available online at www.sciencedirect.com
ScienceDirect
Journal of Sound and Vibration 311 (2008) 683–706
JOURNAL OF SOUND AND VIBRATION
www.elsevier.com/locate/jsvi

Semi-active control of shallow cables with magnetorheological dampers under harmonic axial support motion

Q. Zhou[a,*], S.R.K. Nielsen[b], W.L. Qu[a]

[a]Hubei Key Laboratory of Roadway Bridge and Structure Engineering, Wuhan University of Technology, Wuhan 430070, PR China
[b]Department of Civil Engineering, Aalborg University, Sohngaardsholmsvej 57, DK-9000 Aalborg, Denmark

Received 19 July 2006; received in revised form 6 July 2007; accepted 23 September 2007
Available online 25 October 2007

Abstract

The paper deals with the control of sub- and superharmonic resonances by means of magnetorheological (MR) dampers of an inclined shallow cable caused by parametric excitation from harmonically varying support points. A mechanical model based on the Dahl hysteretic model is used to describe the dynamic property of the MR damper, and the finite difference method is used to discretize the derived governing nonlinear equations of motion of the cable–damper system. Semi-active control strategies are proposed based on the modulated homogeneous friction (SA-1) algorithm and the balance logic (SA-2) algorithm. Four cases are analysed when the circular frequency Ω of the support point motion is in the vicinity of $2\omega_1$, ω_1, $2\omega_1/3$, and $\omega_1/2$, ω_1 being the first in-plane eigenfrequency of the cable. The vibration reduction ability of the MR damper is compared with that of the viscous damper optimally tuned to the first in-plane eigenmode of the cable. The numerical results show that the MR damper with the SA-1 rule and the optimal viscous damper perform similarly to mitigate the vibration of the cable under axial periodic support motion, and, in some cases, the SA-2 rule is more favourable in suppressing the cable vibration compared with the SA-1 rule. In the final analysis, both the MR damper and the viscous damper can effectively mitigate the out-of-plane component of the cable, while having little effect on the reduction of the in-plane response in most cases. Furthermore, when the support motion amplitude is located in a certain range for the case $\Omega \approx 2\omega_1/3$, the original zero out-of-plane vibration of the cable should be changed to the stable in-plane and out-of-plane coupled oscillation by using the optimal passive viscous damper or the MR damper with the SA-1 rule. It is also observed that the vibrations of the cable become chaotic when the cable is supplied with the MR damper using the proposed nonlinear control algorithms.

1. Introduction

Cables are widely used as structural elements in bridges and as supports for masts and towers. Owing to large flexibility, relatively small mass and extremely low inherent damping, cables are prone to excessive vibrations, caused either by direct loads on the cable from wind or a combination of wind and rain, or by the motion of the supported structures, such as bridge decks or towers [1]. In order to mitigate cable vibrations, passive viscous dampers are often mounted at a distance of typically 2–4% of the span from one of the

*Corresponding author. Tel.: +86 27 8716 0361; fax: +86 27 8716 0361.
E-mail address: drzhouqiang@hotmail.com (Q. Zhou).

0022-460X/$ - see front matter © 2007 Elsevier Ltd. All rights reserved.
doi:10.1016/j.jsv.2007.09.022

supports to provide external damping [2]. Kovacs [3] found that the maximum modal damping ratio, which could be provided by the damper, was approximately equal to half the relative distance of the damper from the support. Pacheco et al. [4] numerically developed a "universal estimation curve" of the normalized modal damping ratio versus the normalized damper coefficient. Xu et al. [5] developed a hybrid method based on an orthogonal transformation and a transfer matrix formulation using complex eigenfunctions to study the three-dimensional vibration of inclined cable with oil dampers and to consider the influence of cable sag, cable inclination and damper direction and others. Krenk [6] studied the problem of a taut cable with a concentrated viscous damper and obtained an explicit asymptotic solution for the damping properties in terms of the complex wavenumber. Krenk and Nielsen [7] extended the complex modal analysis to shallow cables and obtained a rather accurate analytical approximation. Main and Jones [8] obtained the range of attainable modal damping ratios and corresponding oscillation frequencies in every mode for a given damper location without approximation. Theoretical and experimental studies of the active control of cable vibrations by axial support motion and active tension control have also been studied [9–11]. However, a number of implementation difficulties remain to be solved before a practical application is possible.

Semi-active dampers can offer active control without requiring the associated large power sources, and moreover, semi-active dampers are fail-safe since they can serve as passive dampers if the power fails. Johnson et al. [12] demonstrated that smart semi-active damping could provide 50–80% reduction in cable response compared with the optimal passive linear damper. It should be noted that only the ideal semi-active damper is used in Johnson's study; hence, the indicated significant reduction could hardly be achieved in reality. However, the study suggests that smart dampers could be an effective replacement for the passive viscous damping of cables. One semi-active device that appears to be particularly promising is the magnetorheological (MR) damper. Ni et al. [13] developed neural network control strategies corresponding to a full-order system model and a reduced-order modal model for the semi-active vibration control of stay cables using MR dampers. Recently, Zhou et al. [14] investigated the three-dimensional vibration control of an inclined sag cable with MR dampers using a semi-active control strategy based on modulated homogeneous friction algorithm, and compared the vibration reduction ability of an MR damper with that of an optimal viscous damper. The results showed that, if only one vibration mode of the cable is excited, the vibration reduction effect by the MR damper is close to that of a viscous damper optimally tuned to this mode; however, if two or more vibration modes of the cable are excited, the MR damper performs better than the viscous damper. Christenson et al. [15] investigated the damping capabilities of a shear MR damper attached to a 12.65 m inclined flat-sag steel cable using H_2/linear quadratic Gaussian clipped control algorithm, and experimental results showed that the MR damper could reduce uncontrolled cable response by more than 50%. The implementation of MR dampers to a cable-stayed bridge and field measurement showed that the MR dampers could effectively mitigate cable vibration caused by wind-and-rain excitation or by other excitation sources [16,17].

For cables used in cable-stayed bridges and TV towers, the primary external excitation is caused by the motion of the support points of the cable rather than by external distributed dynamic loads. Perkins [18] used a first-order perturbation method to study the parametric resonance due to chord elongation from the support excitation using the eigenmodes of the parabolic approximation to the static equilibrium suspension as a function basis. The emphasis was placed on cables with relatively large sag-to-chord-length ratios. Benedettini et al. [19] investigated resonance phenomena of an elastic suspension cable subjected to both external loads and forced support points motions. The corresponding experimental results [20,21] show that strong nonlinear modal coupling between various symmetric and antisymmetric planar and nonplanar modes can exist, when the cable parameters correspond to the first crossover.

Cables used as support of cable-stayed bridges and TV towers are often characterized by a sag-to-chord-length below 0.02, which means that the lowest eigenfrequencies for the in-plane and out-of-plane eigenvibration, ω_1 and ω_2, are very close. The dynamics of the cable are caused by the support point motions at the bridge deck and at the tower. These motions may be decomposed into a component parallel to the chord of the equilibrium suspension, and a component in the orthogonal direction. The chordwise components introduce a chord elongation, which produces parametric excitation in the modal equations of motion in combination with an external excitation of the equations of motion describing the in-plane motion. By contrast, the support point motions in the orthogonal direction merely induce an external excitation of the equations of motion. In case the support point motion is harmonically varying with the circular frequency ω

approximating ω_1, and both the in-plane and out-of-plane components of the cable perform harmonic response with the same circular frequency, we shall talk about harmonic resonance. If ω approx $k\omega_1$, and either the in-plane or the out-of-plane components of the cable perform harmonic resonant vibrations in the fundamental eigenmode, we talk about subharmonic resonance, if $k>1$, and of superharmonic resonance, if $k<1$. The external excitation is the primary excitation during harmonic resonance, whereas the chord elongation and the related parametric excitation are the main reason for sub- and super harmonic responses, although these to some extent are caused by geometric nonlinearities as well. Coupling of the resulting in-plane displacements to large out-of-plane motions is entirely due to geometric nonlinearities. Hence, the complex response pattern observed in sub- and superharmonic responses of inclined cabled is caused by a combination of parametric excitation from the chord elongation, and geometric nonlinearities in the cable response. Since this paper deals with the ability of MR dampers to mitigate sub- and superharmonic responses, the analysis will only consider the parametric excitation from the chord elongation. Nielsen and Kirkegaard [22] investigated the superharmonic response for the case $k=\frac{1}{2}$ and $\frac{2}{3}$ of an elastic cable with small sag using a two-degree-of-freedom modal decomposition based on the lowest in-plane and out-of-plane eigenmodes. Larsen and Nielsen [23] found that up to three stable periodic motions may co-exist for a shallow cable under a harmonic support excitation using a reduced two-degree-of-freedom model and investigated the triggering mechanism for transition between these three states, when the cable is subjected to support motions described by a narrow-banded Gaussian process. Pinto da Costa et al. [24] studied oscillations in the plane of the cable static equilibrium configuration of bridge stay cables subjected to periodic motions of the deck and/or towers using the Galerkin method.

The MR dampers are installed in pairs to the cable to keep the damper system stable, in order to reduce both in-plane and out-of-plane vibration components simultaneously. The finite difference method (FDM) is used to discretize the derived governing nonlinear partial differential equations of the cable–damper system, in which the cable sag, cable inclination, damper direction and other effects are taken into consideration. Semi-active control strategies based on the modulated homogeneous friction algorithm and the balance logic are investigated. Because only the displacement and velocity response of the MR dampers are required, the proposed control rules are easy to implement. Especially, the four cases, where Ω approaches $2\omega_1$, ω_1, $2\omega_1/3$ and $\omega_1/2$, will be analysed. The vibration reduction ability of MR dampers is verified numerically by comparison with the optimal viscous damper tuned to the first in-plane eigenmode of the cable.

2. Mechanics of damper and cable

2.1. Mechanical model of MR damper

Based on experimental evidence, a simple and effective phenomenological model for MR dampers based on the Dahl hysteretic model was developed by Zhou and Qu [25], see in Fig. 1. The Dahl model is adopted to simulate the Coulomb force to reduce the number of parameters in comparison to the Bouc–Wen model [26]. Besides, the modified Dahl model can capture the force-velocity relationship in the low-velocity region with sufficient accuracy.

The damper force is given by

$$F = K_0 x + C_0 \dot{x} + F_d Z - f_0, \tag{1}$$

where K_0 is a stiffness, C_0 is a viscous damping coefficient, F_d is the Coulomb force, and both C_0 and F_d are modulated by the applied magnetic field, x is the displacement of the MR damper, f_0 is the offset force due to

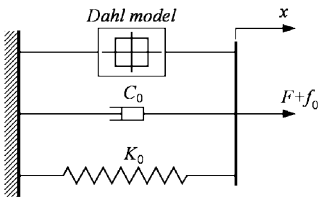

Fig. 1. Modified Dahl model of the MR damper.

the presence of the accumulator. Finally, Z is a nondimensional hysteretic variable governed by

$$\dot{Z} = \sigma\dot{x}(1 - Z\,\mathrm{sgn}(\dot{x})), \tag{2}$$

where σ determines the hysteretic loop shape. In Eq. (1), the term 'F_dZ' corresponds to a Coulomb friction force.

In order to calibrate the modified Dahl model under an applied fluctuating magnetic field, it is necessary to obtain the functional dependence of the model parameters on the applied voltage (or current). When the applied voltage is small enough so that no magnetic saturation occurs in MR fluid, the experimental results show that the steady-state maximum output force generated by the MR damper appears to vary linearly with the applied voltage, and has a nonzero initial value (i.e., at 0 V). Thus C_0 and F_d are related with the applied voltage as follows:

$$C_0 = C_{0s} + C_{0d}u, \quad F_d = F_{ds} + F_{dd}u, \tag{3}$$

where C_{0s} and F_{ds} are the damping coefficient and the Coulomb force of the MR damper at zero field, respectively. u is an intrinsic variable, which determines the dependence of the parameters on the applied voltage V. The relationship between u and V is modelled by the first-order filter [26],

$$\dot{u} = -\eta(u - V), \tag{4}$$

where η reflects the response time of the MR damper, so that larger η implies shorter response time. V is the applied voltage.

Therefore, the proposed MR damper model has a total of 8 parameters (C_{0s}, C_{0d}, F_{ds}, F_{dd}, K_0, σ, f_0 and η) and should be calibrated.

2.2. Equations of motion of cable

The motion equations of the cable with MR dampers are written in a local coordinate system as indicated in Fig. 2. The local x coordinate is taken along the chord line while the y coordinate is in the gravity plane orthogonal to the chord line. The cable is assumed to have a uniform cross-section along its length. Because the profile is shallow, the longitudinal inertial forces and damping force may be neglected. Neglecting flexural rigidity of the cable and external dynamic loading, the nonlinear dynamic equations of motion of the cable with MR dampers can be expressed as [14]

$$\frac{1}{\sqrt{1+y_x^2}}\frac{\partial}{\partial x}\left[(H+h)\frac{\partial w}{\partial x} + hy_x\right] + \sum_{j=1}^{M} F_{dy,j}\delta(x - x_{cj}) = m\frac{\partial^2 w}{\partial t^2} + c_1\frac{\partial w}{\partial t}, \tag{5}$$

$$\frac{1}{\sqrt{1+y_x^2}}\frac{\partial}{\partial x}\left[(H+h)\frac{\partial v}{\partial x}\right] + \sum_{j=1}^{M} F_{dz,j}\delta(x - x_{cj}) = m\frac{\partial^2 v}{\partial t^2} + c_2\frac{\partial v}{\partial t}, \tag{6}$$

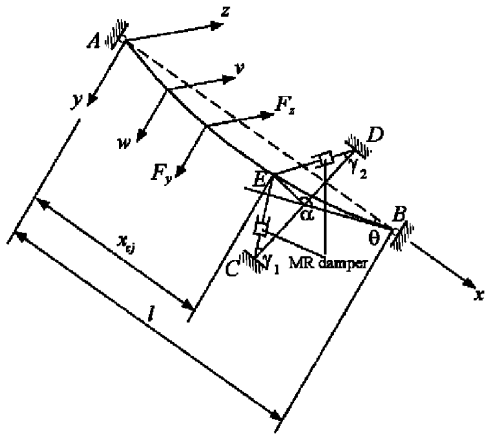

Fig. 2. Schematic diagram of an inclined sag cable with MR dampers.

where H and h are the components of the static and dynamic tension in the x direction, w and v are the dynamic displacement components in the y and z directions measured from the static equilibrium position, $F_{dy,j}$ and $F_{dz,j}$ are the forces generated by the jth MR damper on the cable at the location of x_{cj} in the y and z directions, respectively. l is the cable chord length, M is the total number of MR dampers, δ is Dirac's delta function, m is the mass of the cable per unit length, t is the time, c_1 and c_2 are the in-plane and out-of-plane internal damping coefficients of the cable, respectively. Finally, y_x signifies the partial derivative of the static curve y with respect to x.

It should be noted that the bending stiffness of the cable is neglected in the motion equations. In practice, the position of the damper is relatively close to the lower support, so both the shear force in bending and the rotation of the cable force may be expected to contribute to the transfer of the damper force to the support. Let $\tilde{w}$ denote the displacement of the cable at the damper. Then, the shear force from bending becomes $3\mathrm{EI}\tilde{w}/[x_c^2(l-x_c)]$, where EI is the bending stiffness of the cable, and the shear force from the rotation of the cable becomes $H\tilde{w}/x_c$. Hence the ratio of the former to the latter is $3\mathrm{EI}/[Hx_c(l-x_c)]$. In the vast majority of cable problems, the indicated ratio is quite small, for example, with the data from the numerical example the indicated ratio is about 0.00056. Hence, the effect of the bending stiffness can be ignored for the present case. This is in agreement with a study by Tabatabai and Mehrabi [27], which concludes that the influence of the bending stiffness on the damping performance for the vast majority of actual stay cables is quite unimportant.

Within the shallow cable approximation the static equilibrium curve y of the cable is approximated with the parabola

$$y = \frac{mgl^2\cos\theta}{2H}\frac{x}{l}\left[1-\left(\frac{x}{l}\right)\right], \tag{7}$$

where θ is the angle of chord line with respect to the horizontal plane, see Fig. 2.

The additional dynamic cable tension can be assumed constant along the cable span, and can be expressed as [28]

$$h\left(\frac{\mathrm{d}s}{\mathrm{d}x}\right)^3 = \mathrm{EA}\left[\frac{\partial u}{\partial x}+\frac{\mathrm{d}y}{\mathrm{d}x}\frac{\partial w}{\partial x}+\frac{1}{2}\left(\frac{\partial w}{\partial x}\right)^2+\frac{1}{2}\left(\frac{\partial v}{\partial x}\right)^2\right], \tag{8}$$

where E is Young's modulus, A is the cross sectional area, u is the dynamic displacement components in the x direction and $\mathrm{d}s/\mathrm{d}x$ is the reciprocal of the cosine of the angle subtended to the chord line by the tangent to the profile.

The boundary conditions are

$$u(0,t)=u_1(t), \quad u(l,t)=u_2(t), \tag{9a}$$

$$w(0,t)=w_1(t), \quad w(l,t)=w_2(t), \tag{9b}$$

$$v(0,t)=v_1(t), \quad v(l,t)=v_2(t). \tag{9c}$$

Then, the three components of the displacements u, w and v can be expressed in the form

$$u(x,t)=u_s(x,t), \quad w(x,t)=w_s(x,t)+w_d(x,t), \quad v(x,t)=v_s(x,t)+v_d(x,t), \tag{10}$$

where $u_s(x,t)$, $w_s(x,t)$ and $v_s(x,t)$ are pseudo-static displacements fulfilling the boundary conditions (9), and $w_d(x,t)$ and $v_d(x,t)$ are the residual dynamic displacements fulfilling homogeneous boundary conditions.

The pseudo-static displacement is taken as [29]

$$u_s(x,t)=\left(1-\frac{x}{l}\right)u_1(t)+\frac{x}{l}u_2(t), \tag{11a}$$

$$w_s(x,t)=\left(1-\frac{x}{l}\right)w_1(t)+\frac{x}{l}w_2(t), \tag{11b}$$

$$v_s(x,t)=\left(1-\frac{x}{l}\right)v_1(t)+\frac{x}{l}v_2(t). \tag{11c}$$

Substituting Eqs. (10) and (11) into Eqs. (5) and (6), and omitting $c_1\partial w_s(x,t)/\partial t$ and $c_2\partial v_s(x,t)/\partial t$, Eqs. (5) and (6) can be formulated in the residual dynamic displacements as

$$\frac{1}{\sqrt{1+y_x^2}}\frac{\partial}{\partial x}\left[(H+h)\frac{\partial w_d}{\partial x}+hy_x\right]+\sum_{j=1}^{M}F_{dy,j}\delta(x-x_{cj})=m\frac{\partial^2 w_d}{\partial t^2}+c_1\frac{\partial w_d}{\partial t}+m\frac{\partial^2 w_s}{\partial t^2}, \tag{12}$$

$$\frac{1}{\sqrt{1+y_x^2}}\frac{\partial}{\partial x}\left[(H+h)\frac{\partial v_d}{\partial x}\right]+\sum_{j=1}^{M}F_{dz,j}\delta(x-x_{cj})=m\frac{\partial^2 v_d}{\partial t^2}+c_2\frac{\partial v_d}{\partial t}+m\frac{\partial^2 v_s}{\partial t^2}. \tag{13}$$

Substituting Eqs. (10) and (11) into Eq. (8), performing the integration over l and discarding the differentials of high orders result in

$$\frac{hL_e}{\mathrm{EA}}=(u_2-u_1)+\frac{mg\cos\theta}{H}\int_0^l w_d\,\mathrm{d}x+\frac{1}{2}\int_0^l\left(\frac{\mathrm{d}w_d}{\mathrm{d}x}\right)^2\mathrm{d}x+\frac{1}{2}\int_0^l\left(\frac{\mathrm{d}v_d}{\mathrm{d}x}\right)^2\mathrm{d}x, \tag{14}$$

where L_e denotes the so-called effective cable length [28]

$$L_e=\int_0^l\left(\frac{\mathrm{d}s}{\mathrm{d}x}\right)^3\mathrm{d}x\approx\int_0^l\left(1+\frac{3}{2}\left(\frac{\mathrm{d}y}{\mathrm{d}x}\right)^2\right)\mathrm{d}x=l\left[1+8\left(\frac{f}{l}\right)^2\right], \tag{15}$$

where f is the sag at mid-span

$$f=\frac{mgl^2\cos\theta}{8H}. \tag{16}$$

As seen from Eq. (14), the dynamic cable force accounts for coupling between in-plane and out-of-plane motions as described by Eqs. (12) and (13).

2.3. Damper forces

The displacement and velocity of the MR damper anchored at the points C and D are related to the cable responses at their joint of action E given by the following algebraic equations:

$$\begin{bmatrix}X_C & \dot{X}_C\\ X_D & \dot{X}_D\end{bmatrix}=\begin{bmatrix}\cos\alpha\sin\gamma_1 & -\sin\alpha\sin\gamma_1 & \cos\gamma_1\\ \cos\alpha\sin\gamma_2 & -\sin\alpha\sin\gamma_2 & -\cos\gamma_2\end{bmatrix}\begin{bmatrix}-\sin\theta & 0\\ \cos\theta & 0\\ 0 & 1\end{bmatrix}\begin{bmatrix}w_d(x_{cj}) & \dot{w}_d(x_{cj})\\ v_d(x_{cj}) & \dot{v}_d(x_{cj})\end{bmatrix}, \tag{17}$$

where the angles α, γ_1 and γ_2 defined in Fig. 2 specify the directions CE and DE. It is worthwhile to point out that in Eq. (17) only the residual dynamic response of the cable at point E is affecting the dynamic response of the MR damper, because as shown from Eq. (11) the pseudo-static response of point E (see Fig. 2) is approximately equal to the motion of the dampers anchorage points C and D.

With the displacement and velocity of the MR dampers known, the output force $F_{d,C}$ and $F_{d,D}$ can easily be obtained from Eqs. (1) and (2). Then, the two components of $F_{d,C}$ and $F_{d,D}$ in the y and z directions are given by

$$\begin{bmatrix}F_{dy,C} & F_{dy,D}\\ F_{dz,C} & F_{dz,D}\end{bmatrix}=\begin{bmatrix}-\sin\theta & \cos\theta & 0\\ 0 & 0 & 1\end{bmatrix}\begin{bmatrix}-\cos\alpha\sin\gamma_1 & -\cos\alpha\sin\gamma_2\\ \sin\alpha\sin\gamma_1 & \sin\alpha\sin\gamma_2\\ -\cos\gamma_1 & \cos\gamma_2\end{bmatrix}\begin{bmatrix}F_{d,C} & 0\\ 0 & F_{d,D}\end{bmatrix}. \tag{18}$$

2.4. Discretization of differential equation

The finite difference method is applied to discretize the nonlinear partial differential equations (12) and (13). The cable length is partitioned into n segments of equal length with $x_0=0$ and $x_n=l$. The interval distance

between the ith and $(i+1)$th nodes is $a = l/n$. Using the central difference algorithm, the derivatives of the dynamic displacement component at the ith node can be expressed as

$$\left(\frac{\partial^2 w_d}{\partial x^2}\right)_i = \frac{1}{a^2}(w_{d,i+1} - 2w_{d,i} + w_{d,i-1}),\ \left(\frac{\partial^2 v_d}{\partial x^2}\right)_i = \frac{1}{a^2}(v_{d,i+1} - 2v_{d,i} + v_{d,i-1}). \tag{19}$$

The last two terms of the right-hand side of Eq. (14) can be given as [14]

$$\frac{1}{2}\int_0^l \left(\frac{\mathrm{d}w_d}{\mathrm{d}x}\right)^2 \mathrm{d}x = \frac{1}{a}\left[\sum_{j=1}^{n-1} w_{d,j}^2 - \sum_{j=1}^{n-2} w_{d,j}w_{d,j+1}\right], \tag{20a}$$

$$\frac{1}{2}\int_0^l \left(\frac{\mathrm{d}v_d}{\mathrm{d}x}\right)^2 \mathrm{d}x = \frac{1}{a}\left[\sum_{j=1}^{n-1} v_{d,j}^2 - \sum_{j=1}^{n-2} v_{d,j}v_{d,j+1}\right]. \tag{20b}$$

Substituting Eqs. (19), (20) into Eqs. (12–14) yields the following ordinary differential equations:

$$\begin{aligned} &m\ddot{w}_{d,i} + c_1\dot{w}_{d,i} + f_{1,i} - \sum_{j=1}^{M} F_{dy,j}\delta(x - x_{cj}) + \frac{1}{\sqrt{1+y_{x,i}^2}}\frac{\lambda^2 H}{l^3} a \sum_{j=1}^{n-1} w_{d,j} \\ &\quad + \frac{1}{\sqrt{1+y_{x,i}^2}}\left[H + \frac{\mathrm{EA}}{L_e}(u_2 - u_1)\right]\frac{1}{a^2}(w_{d,i+1} - 2w_{d,i} + w_{d,i-1}) \\ &= -m\frac{\partial^2 w_s}{\partial t^2} - \frac{1}{\sqrt{1+y_{x,i}^2}}\frac{mg\cos\theta}{H}\frac{\mathrm{EA}}{L_e}(u_2 - u_1), \end{aligned} \tag{21}$$

$$\begin{aligned} &m\ddot{v}_{d,i} + c_1\dot{v}_{d,i} + f_{2,i} - \sum_{j=1}^{M} F_{dz,j}\delta(x - x_{cj}) \\ &\quad + \frac{1}{\sqrt{1+y_{x,i}^2}}\left[H + \frac{\mathrm{EA}}{L_e}(u_2 - u_1)\right]\frac{1}{a^2}(v_{d,i+1} - 2v_{d,i} + v_{d,i-1}) = -m\frac{\partial^2 v_s}{\partial t^2}, \end{aligned} \tag{22}$$

where $f_{1,i}$ and $f_{2,i}$ are nonlinear terms given as

$$\begin{aligned} f_{1,i} = &-\frac{1}{\sqrt{1+y_{x,i}^2}}\frac{\mathrm{EA}}{aL_e}\frac{mg\cos\theta}{H}(w_{d,i+1} - 2w_{d,i} + w_{d,i-1})\sum_{j=1}^{n-1} w_{d,j} \\ &-\frac{1}{\sqrt{1+y_{x,i}^2}}\frac{\mathrm{EA}}{a^3L_e}(w_{d,i+1} - 2w_{d,i} + w_{d,i-1})\left[\left[\sum_{j=1}^{n-1} w_{d,j}^2 - \sum_{j=1}^{n-2} w_{d,j}w_{d,j+1}\right] + \left[\sum_{j=1}^{n-1} v_{d,j}^2 - \sum_{j=1}^{n-2} v_{d,j}v_{d,j+1}\right]\right] \\ &+\frac{1}{\sqrt{1+y_{x,i}^2}}\frac{\mathrm{EA}}{aL_e}\frac{mg\cos\theta}{H}\left[\left[\sum_{j=1}^{n-1} w_{d,j}^2 - \sum_{j=1}^{n-2} w_{d,j}w_{d,j+1}\right] + \left[\sum_{j=1}^{n-1} v_{d,j}^2 - \sum_{j=1}^{n-2} v_{d,j}v_{d,j+1}\right]\right], \end{aligned} \tag{23}$$

$$\begin{aligned} f_{2,i} = &-\frac{1}{\sqrt{1+y_{x,i}^2}}\frac{\mathrm{EA}}{aL_e}\frac{mg\cos\theta}{H}(v_{d,i+1} - 2v_{d,i} + v_{d,i-1})\sum_{j=1}^{n-1} w_{d,j} \\ &-\frac{1}{\sqrt{1+y_{x,i}^2}}\frac{\mathrm{EA}}{a^3L_e}(v_{d,i+1} - 2v_{d,i} + v_{d,i-1})\left[\left[\sum_{j=1}^{n-1} w_{d,j}^2 - \sum_{j=1}^{n-2} w_{d,j}w_{d,j+1}\right] + \left[\sum_{j=1}^{n-1} v_{d,j}^2 - \sum_{j=1}^{n-2} v_{d,j}v_{d,j+1}\right]\right], \end{aligned} \tag{24}$$

λ^2 is the nondimensional Irvine parameter for sag extensibility given as [28]

$$\lambda^2 = \left(\frac{mgl\cos\theta}{H}\right)^2 l\frac{EA}{HL_e}. \tag{25}$$

The nonlinear equations of dynamic equilibrium (21) and (22) are solved by an incremental-iterative algorithm based on the Newmark beta algorithm in combination with Newton–Raphson iteration [30].

3. Control strategies

3.1. Semi-active control based on modulated homogeneous friction algorithm (SA-1)

Essentially, the MR damper can be considered as a variable friction damper. Inaudi [31] proposed a control strategy for the design of semi-active friction controllers, the so-called modulated homogeneous friction algorithm, which produces dissipation of energy per cycle equal to the square of the deformation amplitude and maximum dissipation efficiency for the resistance–force level proportional to the deformation. In this control algorithm, the control friction force for the ith MR damper is proportional to the absolute value of the previous local peak of the damper deformation signal, that is,

$$N_i = \beta_i\left|P[X_i(t)]\right|, \tag{26}$$

where $\beta_i > 0$ is the controller gain, $P[X_i(t)]$ is the local peak of the displacement of the MR damper prior to the current time t, defined as

$$P[X_i(t)] = X_i(t-s), \quad s = \left\{\min\ \bar{t} \geqslant 0 : \frac{dX_i(t-\bar{t})}{dt} = 0\right\}, \tag{27}$$

s is time interval between the immediate previous local peak and the current time t. After N_i is obtained, and if η is large enough, from Eq. (4) it can be assumed that u is approximately equal to V, so according to Eq. (3b), the required voltage for the MR damper is given by

$$V_{i,\text{need}} = \frac{N_i - F_{ds,i}}{F_{dd,i}}. \tag{28}$$

The applied voltage to the MR damper has a range from 0 to $V_{\max}$. So the semi-active control strategy takes the following form:

$$V_i = \begin{cases} 0, & V_{i,\text{ need}} < 0, \\ V_{i,\text{ need}}, & 0 \leqslant V_{i,\text{need}} \leqslant V_{\max}, \\ V_{\max}, & V_{i,\text{need}} > V_{\max}. \end{cases} \tag{29}$$

3.2. Semi-active control based on balance logic algorithm (SA-2)

In order to control machinery foundations or vehicles using semi-active dry friction damping, Stammers and Sireteanu [32] proposed the so-called balance logic algorithm. The basic idea of this strategy is to reduce the elastic and damping force resultants across the controlled object by forcing the damping force to balance the elastic force, when these forces act in the opposite direction, i.e., when $x\dot{x} < 0$, and by setting the damping force to a minimum value when $x\dot{x} > 0$. The controllable friction force for the ith MR damper can then be expressed as

$$N_i = \begin{cases} \beta_i|X_i|, & X_i\dot{X}_i \leqslant 0, \\ 0, & X_i\dot{X}_i > 0, \end{cases} \tag{30}$$

where X and $\dot{X}$ are displacement and velocity of the ith MR damper, and $\beta_i > 0$ is the controller gain. Given N_i, the required voltage for the MR damper can be obtained using Eqs. (28) and (29).

It should be noted that the main purpose of using the SA-1 rule is to dissipate as much as possible of the input energy, while the main purpose of using the SA-2 rule is to reduce or balance the elastic force acting on the cable.

From Eqs. (26) and (30), it can be seen that the implementation of the indicated control strategies only requires the measurements of the displacement and the velocity of the MR dampers.

Compared with other control algorithms based on the optimal control theory [33], such as the linear quadratic regulator (LQR) algorithm, and the instantaneous optimal control algorithm, the proposed semi-active control algorithm has some advantages. The most important merit is the easy implementation because only the local dynamic responses (displacement and velocity) of the MR dampers are required. However, the controller gain should be properly determined through numerical parameter studies for a given structure.

4. Simplified model

For simplicity, the cable with a pair of dampers at $x = x_c$ with the same dynamic characteristics is considered. The in-plane and out-of-plane displacement of the cable can be approximated using a finite series

$$w_d(x,t) = \sum_{j=1}^{n} p_j(t)\phi_j(x), \quad v_d(x,t) = \sum_{j=1}^{n} q_j(t)\phi_j(x), \tag{31}$$

where the $p_j(t)$ and $q_j(t)$ are generalized displacements and the $\phi_j(x)$ are a set of shape functions that are continuous with piecewise continuous slope and that satisfy the geometric boundary conditions. Johnson et al. [34] has pointed out that if only sinusoidal shape functions are adopted, then hundreds of shape functions are required to obtain a true solution. While using a linear combination of the static deflection shape and the first sine term, the obtained solution closely approximates the first mode of the cable–damper system. Therefore, it may be worthwhile to point out that in the simplified analysis the shape function based on the deflection due to a static unit force at the damper location should be included to avoid some unreliable conclusions. In this analysis, only two shape functions are used as [34]

$$\phi_1(x) = \begin{cases} x/x_c & 0 \leqslant x \leqslant x_c \\ (l-x)/(l-x_c) & x_c \leqslant x \leqslant l \end{cases}, \quad \phi_2(x) = \sin\frac{\pi x}{l}, \tag{32}$$

where $\phi_1(x)$ is the normalized deflection due to a static force at the damper location and $\phi_2(x)$ is the first out-of-plane eigenmode of a taut cable (Irvine parameter $\lambda^2 = 0$). Substituting Eqs. (31) and (32) into Eqs. (12)–(14), using a standard Galerkin approach gives

$$\begin{bmatrix} m[A]_{2\times2} & [0]_{2\times2} \\ [0]_{2\times2} & m[A]_{2\times2} \end{bmatrix} \{\ddot{P}\} + \begin{bmatrix} c_1[A]_{2\times2} & [0]_{2\times2} \\ [0]_{2\times2} & c_2[A]_{2\times2} \end{bmatrix} \{\dot{P}\} + (H+h) \begin{bmatrix} [B]_{2\times2} & [0]_{2\times2} \\ [0]_{2\times2} & [B]_{2\times2} \end{bmatrix} \{P\} + h\frac{mg\cos\theta}{H}\{d\}_{4\times1} - \begin{Bmatrix} F_{dy}\{g\}_{2\times1} \\ F_{dz}\{g\}_{2\times1} \end{Bmatrix} = \{0\}_{4\times1}, \tag{33}$$

where $(\cdot)$ denotes partial derivatives with respect to t, F_{dy} and F_{dz} are the resultant forces generated by dampers in the y and z directions, respectively, and

$$[A]_{2\times2} = \begin{bmatrix} \dfrac{l}{3} & \dfrac{\sin\pi\zeta \quad l}{\zeta(1-\zeta)\pi^2} \\ \dfrac{\sin\pi\zeta \quad l}{\zeta(1-\zeta)\pi^2} & \dfrac{l}{2} \end{bmatrix}, \quad [B]_{2\times2} = \begin{bmatrix} \dfrac{1}{l\zeta(1-\zeta)} & \dfrac{\sin\pi\zeta}{l\zeta(1-\zeta)} \\ \dfrac{\sin\pi\zeta}{l\zeta(1-\zeta)} & \dfrac{\pi^2}{2l} \end{bmatrix}, \tag{34a}$$

$$\{P\} = \begin{bmatrix} p_1 & p_2 & q_1 & q_2 \end{bmatrix}^{\mathrm{T}}, \quad \{d\} = \begin{bmatrix} l/2 & 2l/\pi & 0 & 0 \end{bmatrix}^{\mathrm{T}}, \quad \{g\} = \begin{bmatrix} 1 & \sin\pi\zeta \end{bmatrix}^{\mathrm{T}}, \tag{34b}$$

$$h = \frac{\mathrm{EA}}{l}\left[u_2 - u_1 + \frac{mg\cos\theta}{H}\{d\}^{\mathrm{T}}\{P\} + \frac{\mathrm{EA}}{2l}\{P\}^{\mathrm{T}} \begin{bmatrix} [B]_{2\times2} & [0]_{2\times2} \\ [0]_{2\times2} & [B]_{2\times2} \end{bmatrix} \{P\}\right], \quad \zeta = x_c/l. \tag{34c}$$

If neglecting all second- and third-order terms, in other words, ignoring the in-plane and out-of-plane components interaction terms, Eq. (33) can be reduced to

$$\begin{bmatrix} m[A]_{2\times2} & [0]_{2\times2} \\ [0]_{2\times2} & m[A]_{2\times2} \end{bmatrix}\{\ddot{P}\} + \begin{bmatrix} c_1[A]_{2\times2} & [0]_{2\times2} \\ [0]_{2\times2} & c_2[A]_{2\times2} \end{bmatrix}\{\dot{P}\} + \left(H + \frac{EA}{l}u\right)\begin{bmatrix} [B]_{2\times2} & [0]_{2\times2} \\ [0]_{2\times2} & [B]_{2\times2} \end{bmatrix}\{P\} + \frac{EA}{l}\left(\frac{mg\cos\theta}{H}\right)^2\begin{bmatrix} [C]_{2\times2} & [0]_{2\times2} \\ [0]_{2\times2} & [0]_{2\times2} \end{bmatrix}\{P\} - \begin{Bmatrix} F_{dy}\{g\}_{2\times1} \\ F_{dz}\{g\}_{2\times1} \end{Bmatrix} = -\frac{EA}{l}\frac{mg\cos\theta}{H}(u_2-u_1)\{d\}_{4\times1}, \tag{35}$$

where

$$[C]_{2\times2} = \begin{bmatrix} l^2/4 & l^2/\pi \\ l^2/\pi & 4l^2/\pi^2 \end{bmatrix}. \tag{36}$$

Eq. (35) can be approximately considered as a Mathieu-type equation. The parametric excitation takes place in the stiffness term via the chord elongation u_2–u_1.

Ideal variable viscous dampers are considered, whose adjustable damping coefficient $\bar{C}$ is either C_{vvd} or zero according to some control rule. Here, the balance logic control rule is selected, and the gain coefficient β is assumed to be positive infinite for simplification, that is,

$$\bar{C} = \begin{cases} C_{vvd}, & X\dot{X} \leqslant 0, \\ 0, & X\dot{X} > 0. \end{cases} \tag{37}$$

In general, the direction of the installed dampers is set to be $\alpha+\theta = 90^\circ$ and $\gamma_1 = \gamma_2 = 45^\circ$, which can provide the same maximum modal damping ratios to both planes vibration modes [35]. Substituting these angles into Eqs. (17) and (18), the resultant damping forces generated by variable viscous dampers in the y and z directions are given by

$$\begin{Bmatrix} F_{dy} \\ F_{dz} \end{Bmatrix} = \begin{bmatrix} -\frac{1}{2}(\bar{C}_C + \bar{C}_D) & \frac{1}{2}(\bar{C}_C - \bar{C}_D) \\ \frac{1}{2}(\bar{C}_C - \bar{C}_D) & -\frac{1}{2}(\bar{C}_C + \bar{C}_D) \end{bmatrix}\begin{Bmatrix} \dot{p}_1 + \dot{p}_2\sin\pi\zeta \\ \dot{q}_1 + \dot{q}_2\sin\pi\zeta \end{Bmatrix}, \tag{38}$$

where $\bar{C}_C$ and $\bar{C}_D$ are the viscous coefficients of dampers anchored at the points C and D, respectively. According to Eq. (37), these two coefficients are defined as

$$\bar{C}_C = \begin{cases} C_{vvd}, & (\bar{w}-\bar{v})(\dot{\bar{w}}-\dot{\bar{v}}) \leqslant 0, \\ 0, & (\bar{w}-\bar{v})(\dot{\bar{w}}-\dot{\bar{v}}) > 0, \end{cases} \quad \bar{C}_D = \begin{cases} C_{vvd}, & (\bar{w}+\bar{v})(\dot{\bar{w}}+\dot{\bar{v}}) \leqslant 0, \\ 0, & (\bar{w}+\bar{v})(\dot{\bar{w}}+\dot{\bar{v}}) > 0, \end{cases} \tag{39}$$

where

$$\begin{bmatrix} \bar{w} & \dot{\bar{w}} \\ \bar{v} & \dot{\bar{v}} \end{bmatrix} = \begin{bmatrix} 1 & \sin\pi\zeta & 0 & 0 \\ 0 & 0 & 1 & \sin\pi\zeta \end{bmatrix}\begin{bmatrix} \{P\} & \{\dot{P}\} \end{bmatrix}. \tag{40}$$

When a pair of passive viscous dampers with the same viscous coefficient is used, Eq. (38) can be reduced to

$$\begin{Bmatrix} F_{dy} \\ F_{dz} \end{Bmatrix} = \begin{bmatrix} -\bar{C} & 0 \\ 0 & -\bar{C} \end{bmatrix}\begin{Bmatrix} \dot{p}_1 + \dot{p}_2\sin\pi\zeta \\ \dot{q}_1 + \dot{q}_2\sin\pi\zeta \end{Bmatrix}. \tag{41}$$

After $\{P\}$ is solved, the in-plane and out-of-plane displacement at the midpoint of the cable can be obtained from

$$w_d|_{x=\frac{l}{2}} = \frac{0.5}{1-\zeta}p_1 + p_2, \quad v_d|_{x=\frac{l}{2}} = \frac{0.5}{1-\zeta}q_1 + q_2. \tag{42}$$

Table 1
Natural frequencies of in-plane and out-of-plane modes of cable

Mode order	Natural circular frequency (rad/s)		Remark
	In-plane	Out-of-plane	
1	3.201	3.148	Symmetric mode
2	6.295	6.295	Antisymmetric mode
3	9.445	9.443	Symmetric mode
4	12.590	12.590	Antisymmetric mode
5	15.738	15.738	Symmetric mode
6	18.886	18.886	Antisymmetric mode

Table 2
Parameters of MR damper

C_{0s} (N s/m)	C_{0d} (N s/m/V)	F_{ds} (N)	F_{dd} (N/V)	K_0 (N/m)	σ (m^{-1})	f_0 (N)	η (s^{-1})
2.4×10^4	3.6×10^3	2.0×10^3	1.5×10^4	3.0×10^4	5.0×10^4	0.0	200

5. Numerical simulations

The data of the considered cable refers to the longest stay in the cable-stayed bridge across the Øresund between Denmark and Sweden. The stiffness of the cable is $EA = 2.17\times10^9$ N, and the equilibrium force $H = 5.5\times10^6$ N. The chord length is 260.0 m, the cable mass per unit length is $m = 81.05$ kg/m and the inclination θ is 30.4°. The nondimensional Irvine parameter is $\lambda^2 = 0.414$.

The lower circular eigenfrequencies of the in-plane and out-of-plane modes are given in Table 1. The modal damping ratios of the in-plane and out-of-plane modes are both taken as 1.0%, and the corresponding viscous damping constants of in-plane and out-of-plane vibrations, c_1 and c_2, can be obtained by

$$c_1 = 2\xi\omega_1 m, \quad c_2 = 2\xi\omega_2 m. \tag{43}$$

To achieve the maximum possible reduction of dynamic response of the cable in both in-plane and out-of-plane vibrations, a pair of MR dampers are installed symmetrically to the cable at the position $(l–x_{cj}) = l/30$, with the damper directions $\gamma_1 = \gamma_2 = 45°$, and $\alpha = 59.6°$. The angle α is chosen in a way that the damper forces are acting normal to the chord line of the inclined cable, which can be regarded as an optimum direction [35]. Based on the model test performance in Ref. [25], the selected parameters of the MR damper are listed in Table 2, and the adjustable voltage range is from 0 to –7 V.

To validate the vibration reduction effect of the MR dampers, the dynamic response analysis with an optimal viscous damper is also performed. The installation pattern of the viscous dampers is the same as that of the MR dampers. The optimal normalized damper size for the first in-plane mode is given by [4,6]

$$C_{\text{opt}} = \frac{\sqrt{Hm}}{\pi x_j/l} \approx 0.1\frac{ml\omega_1}{x_j/l}. \tag{44}$$

Then, the optimum damping coefficient C_{opt} is taken as 2.024×10^5 N s/m.

After extensive numerical analysis, it can be found that there exists an optimal controller gain β in semi-active control rule. For the given cable, the optimal gain β is 5.0×10^5 for SA-1 and 6.0×10^5 for SA-2, respectively, and both optimal gains are fixed in the following research.

The cable is divided into 30 or 60 elements to check convergence. The corresponding subharmonic displacement response at the mid-span of the cable with MR dampers subjected to a harmonic support point motion is shown in Fig. 3. It can be seen that calculation with 30 elements provides sufficient accuracy, which henceforth will be used in the analysis.

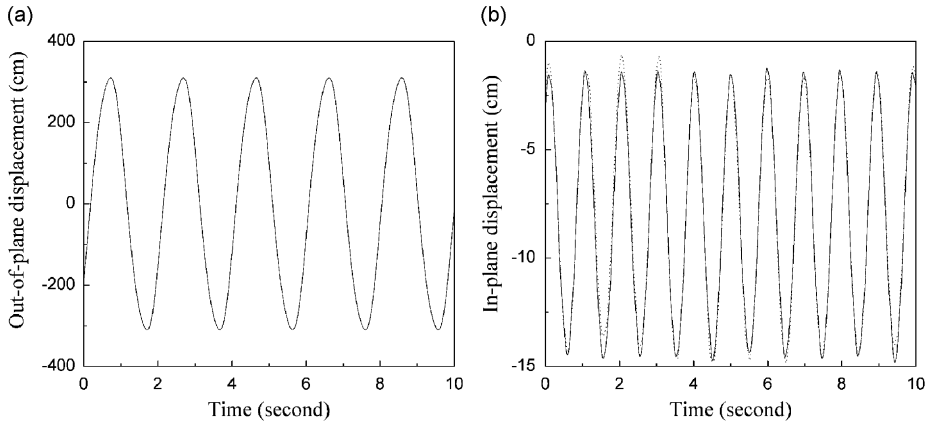

Fig. 3. Displacement response at the midpoint as a function of number of elements. $U = 0.15\,\text{m}$, $\Omega = 2\omega_1$. Solid line: $n = 30$. Dashed line: $n = 60$.

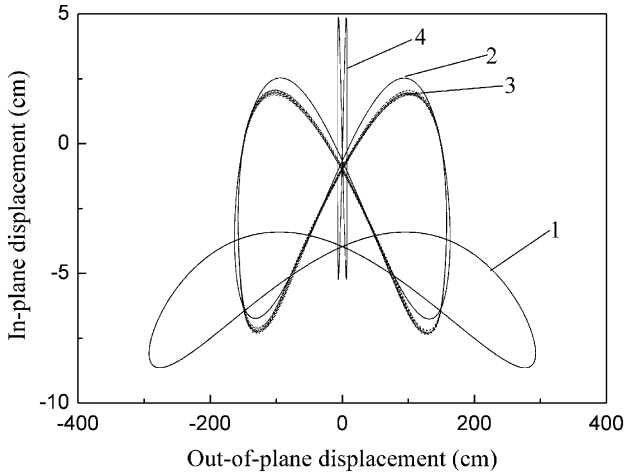

Fig. 4. Subharmonic response, $k = 2$. Trajectories at the midpoint. $U = 0.08\,\text{m}$, $\Omega = 2\omega_1$. 1: original cable. 2: optimal viscous damper. 3: MR damper using SA-1. 4: MR damper using SA-2.

The chordwise elongation is produced by applying the harmonic motion at support point B, while the other support point is set to zero.

The initial out-of-plane displacement in Eq. (22) is taken as

$$v_i|_{t=0} = v_{d,i}|_{t=0} = d_{\text{ms}} \sin(\pi x_i/l), \tag{45}$$

where x_i is the coordinate of the ith node in the x direction and d_{ms} is the out-of-plane displacement at the mid-span of the cable. In the following analysis d_{ms} is set to be 1.0 m.

5.1. Subharmonic response, $\Omega \approx 2\omega_1$

When the out-of-plane motion of the cable is prevented, Zhou et al. [14] found that when the harmonic frequency of the chord elongation is in the neighbourhood of two times the first natural frequency of the cable, and the amplitude of the chord elongation does not exceed a certain threshold value, the MR damper with the SA-1 control rule can prevent the development of subharmonic excitations, whereas the viscous damper fails to do so. However, if the motion amplitude exceeds the said threshold value, large subharmonic vibrations occur in both cases.

Therefore, the focus in this study will be on the coupled motion between the in-plane and the out-of-plane components. In Fig. 4, the trajectory at the midpoint of the undamped cables has been shown as curve 1. As seen, the out-of-plane component performs large harmonic vibrations with half the frequency of the excitation, indicating a subharmonic resonance of the order $k = 2$. By contrast the in-plane component is performing harmonic oscillations with the same frequency as the excitations, making the trajectory of the shape as an infinity sign possible. The amplitude of the in-plane harmonic response is small, because the excitation frequency is far away from the fundamental resonance frequency.

At first, the amplitude U of the chord elongation is chosen as 0.08 m. The trajectories of w_d and v_d at the midpoint of the cable are shown in Fig. 4. It can be seen that both the viscous damper and the MR damper can suppress the out-of-plane vibration to some extent. In the case of original cable without dampers, the peak value of the out-of-plane component $v_{\max}$ is 292.7 cm. For the cable with the optimal viscous dampers and with the MR dampers using the SA-1 control rule, $v_{\max}$ is reduced to 163.2 and 157.9 cm, respectively, which means that the dampers can provide about 45% reduction compared with the original cable. Compared with the viscous damper, the MR damper with the SA-1 rule only provides 3.2% reduction effect. However, when adopting the SA-2 control rule, $v_{\max}$ is only 7.3 cm, which are only about 1/40 compared with $v_{\max}$ of the undamped cable. On the other hand, the peak-to-peak value of the in-plane response is amplified after the dampers are installed. For the original cable, the value is about 5.2 cm, while it is increased to 9.3 cm for the viscous damper, 9.4 cm for the MR damper with the SA-1 rule and 10.1 cm for the MR damper with the SA-2 rule. However, the amplitude of the in-plane response is two orders of magnitude less than that of the out-of-plane component. Therefore, the increase of the in-plane peak-to-peak value has minute influence on the control effect of the damper. Fig. 5 shows the force–displacement relation of the MR damper anchored at the points C and E with different control rules. It can be seen that the MR damper with the SA-1 rule can dissipate much more energy than that with the SA-2 rule. It should be noted that the steady-state variable range of the applied voltage for the MR damper is 2.0–2.7 V by the SA-1 rule and 0–0.035 V by the SA-2 rule, respectively, that is, if the varied level of the applied voltage is small, then the force–displacement curves of the semi-active MR damper look like that of the MR damper with a constant applied voltage.

It should be noted that the viscous damper is tuned to the first in-plane eigenmode of the cable. As mentioned above, for a cable with a sag-to-chord-length ratio below 0.02, the natural frequencies for the in-plane and out-of-plane vibrations are pairwise close (see Table 1). In other words, the viscous damper is also tuned to the first out-of-plane eigenmode simultaneously. When $\Omega = 2\omega_1$, the out-of-plane vibration is dominated by the first eigenmode. In view of this, the viscous damper was expected to provide a more satisfactory vibration reduction effect than observed in Fig. 4. By contrast, the MR dampers with the SA-2 rule provide a 95.5% reduction compared with the viscous damper. In order to explain this, an ideal variable viscous damper mentioned in Section 4 is used with $C_{\mathrm{vvd}} = C_{\mathrm{opt}}$.

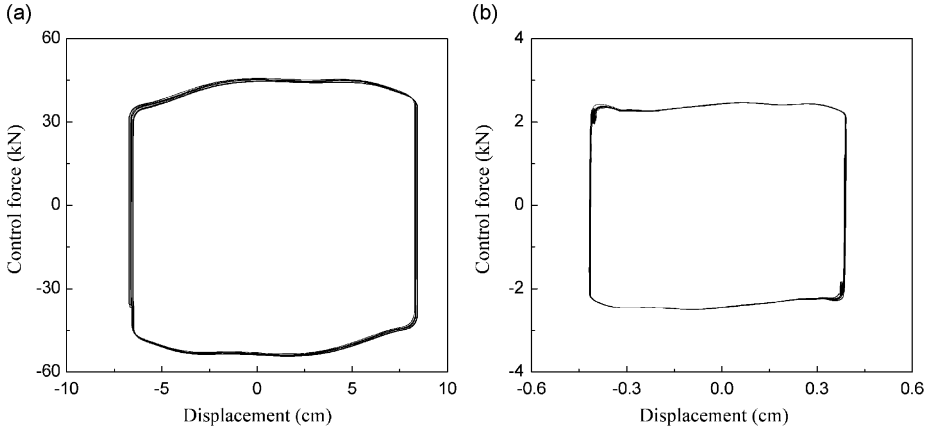

Fig. 5. Subharmonic response, $k = 2$. Force–displacement relationship of the MR damper linking the points C and E. $U = 0.08$ m, $\Omega = 2\omega_1$. (a) SA-1 rule; (b) SA-2 rule.

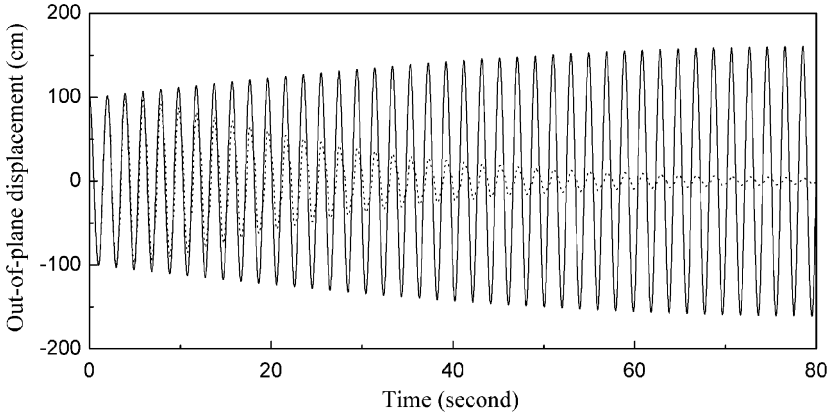

Fig. 6. Subharmonic response, $k = 2$. Displacement response at the midpoint. $U = 0.08$ m, $\Omega = 2\omega_1$. Solid line: optimal passive viscous damper. Dashed line: ideal variable viscous damper.

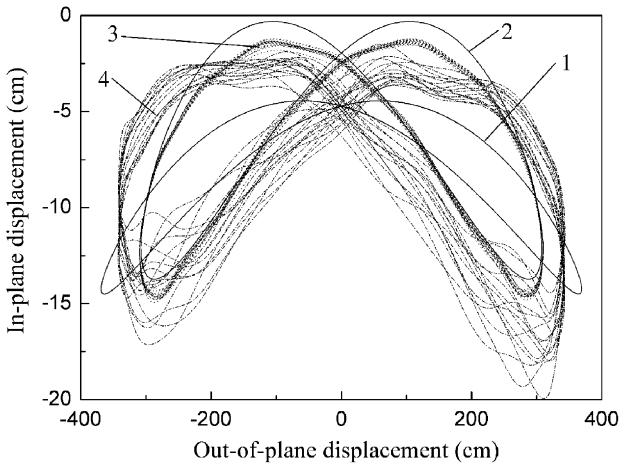

Fig. 7. Subharmonic response, $k = 2$. Trajectories at the midpoint. $U = 0.15$ m, $\Omega = 2\omega_1$. 1: original cable. 2: optimal viscous damper. 3: MR damper using SA-1. 4: MR damper using SA-2.

The out-of-plane responses at the mid-span of the cable with the variable viscous dampers and with the passive viscous dampers are shown in Fig. 6. It can be seen that the variable viscous damper works very well, and the out-of-plane component will disappear eventually. The point is that the variable viscous damper and the passive optimal viscous damper are two different methods to reduce the dynamic response. The main function of the former is to reduce or balance the elastic force acting on the cable, while that of the latter is to dissipate as much as possible of the input energy. Although the passive optimal viscous damper can dissipate much more input energy than the variable viscous damper, the latter is far superior to the former as can be seen from Fig. 6. In other words, the control strategy to balance the elastic force acting on the cable is more effective than to dissipate the input energy. When the balance logic algorithm is used, the controllable force should be zero in case of $x\dot{x} < 0$ to achieve the best control effect, see Eq. (30). For the MR damper, even if the applied voltage is zero, the output force is rarely zero, whereas the output force produced by the ideal variable viscous damper can be zero. Therefore, in this respect, the ideal variable viscous damper is superior to the MR damper when using the SA-2 rule.

Next, the amplitude U is increased to 0.15 m. The trajectories at the midpoint of the cable are shown in Fig. 7. It can be seen that for the undamped cable, $v_{\max}$ is 369.0 cm. For the cable with the optimal viscous dampers and with the MR dampers using the SA-1 and SA-2 control rules, $v_{\max}$ is reduced to 307.5, 310.0 and

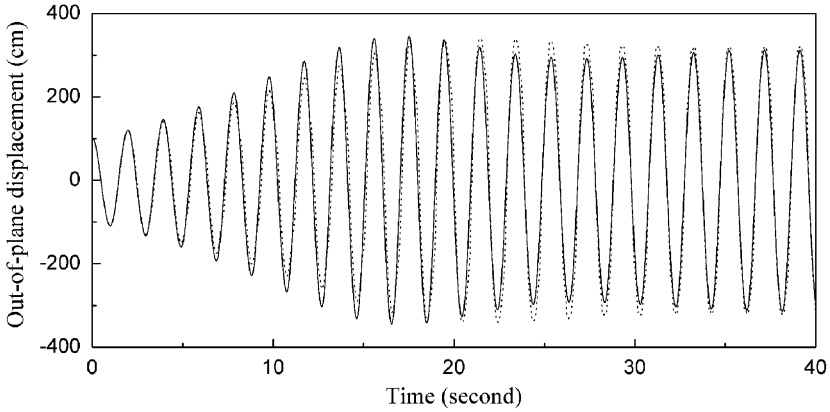

Fig. 8. Subharmonic response, $k = 2$. Displacement response at the midpoint. $U = 0.15$ m, $\Omega = 2\omega_1$. Solid line: optimal passive viscous damper. Dashed line: ideal variable viscous damper.

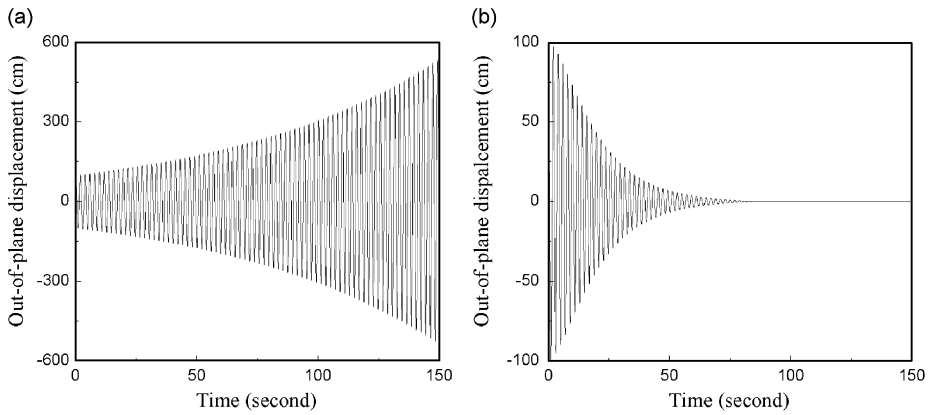

Fig. 9. Solution of Mathieu–Hill equation using different damper. $U = 0.08$ m, $\Omega = 2\omega_1$. (a) Passive viscous damper. (b) Ideal variable viscous damper.

342.8 cm, respectively. Compared with the original cable, the viscous damper and the MR damper with the SA-1 rule can provide about 16% reduction, while the MR damper with the SA-2 rule only offers 7% reduction. It can be seen that the peak-to-peak value of the in-plane component increases again. Further, the multilined appearance of the trajectories for the SA-1 and SA-2 rules suggests some chaotic response of the cable in these control cases. Fig. 8 shows the out-of-plane response at the mid-span with the variable viscous dampers and the passive viscous dampers, respectively. It can be seen that the vibration reduction effect by the balancing elastic force method and that by the dissipating input energy method is very close.

Using the given data, Fig. 9 shows the out-of-plane displacement at the midpoint by solving the Mathieu type Eq. (35) with the ideal variable viscous damper and the optimal passive viscous damper, when the amplitude of the chord elongation is 0.08 m. It can be seen that the variable viscous damper makes the vibration decay while the passive viscous damper gives an unstable solution. If the excitation amplitude is further increased, then both dampers will lead to unstable solutions. Therefore, this implies that the balance logic rule will decrease the unstable range of the Mathieu equation compared with the energy dissipation rule. So this may be a physical explanation as to why the SA-2 rule is much better than the SA-1 rule under smaller excitation amplitudes while both rules give similar control effect under larger excitation amplitudes. It should be noted that the 'unstable' in here only means that the solution of Eq. (35) is divergent and does not stand for the actual response of the cable–damper system. In fact, when the nonlinear terms are considered, Eq. (33) will give both stable periodic solutions for the cable with variable and passive viscous dampers with $U = 0.08$ and 0.15 m.

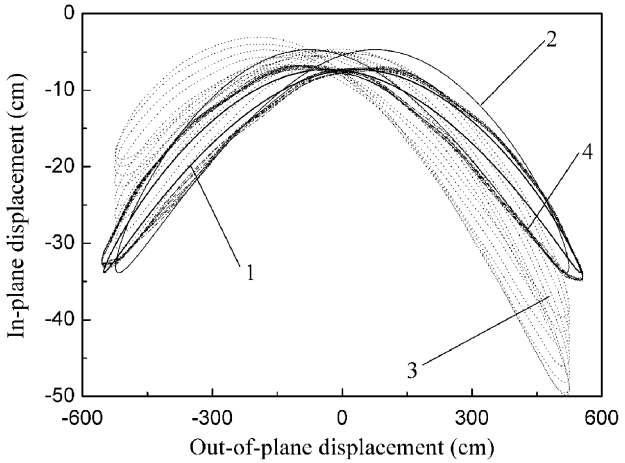

Fig. 10. Subharmonic response, $k = 2$. Trajectories at the midpoint. $U = 0.40$ m, $\Omega = 2\omega_1$. 1: original cable. 2: optimal viscous damper. 3: MR damper using SA-1. 4: MR damper using SA-2.

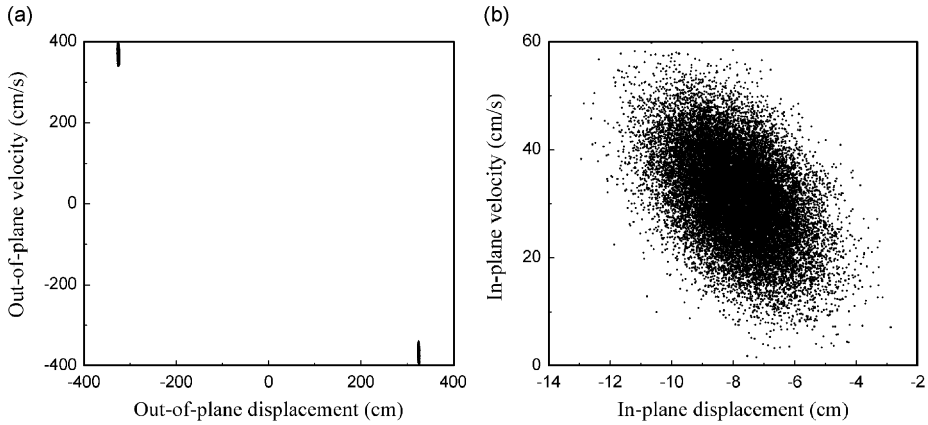

Fig. 11. Subharmonic response, $k = 2$. Poincaré map at the midpoint response with the MR damper using the SA-2 rule. $U = 0.15$ m, $\Omega = 2\omega_1$.

Finally, the amplitude U is increased to 0.40 m. The trajectories at the midpoint of the cable are illustrated in Fig. 10. It can be seen that the maximum values of the out-of-plane vibration of the cable without the damper, with the viscous damper and with the MR damper using the different control strategies are rather close. Hence, neither the viscous damper nor the MR damper has any capability to dissipate the dynamic response of the cable in this case. Again, some chaotic behaviour is noticed for the various control strategies of the MR dampers.

From the FDM equations (21) and (22), it can be observed that with the increase of the support motion amplitude, the dynamic response of the original cable increases. However, the position where the dampers are installed approaches closely the end of the cable; consequently, the output force generated by the dampers is restricted. So, on the whole, the vibration reduction effect provided by the dampers attenuates with the increase of the excitation amplitude, as shown in Figs. 4 and 7.

From Figs. 4 and 7 it is also concluded that the vibration reduction effect by the MR damper with the SA-1 rule is close to that by the viscous damper. The reason is that according to the maximum energy dissipation principle the viscous damper is tuned to the first eigenmode of the cable, which is the main mode of the out-of-plane vibration, and the main principle of the SA-1 rule is to absorb as much as possible the input energy.

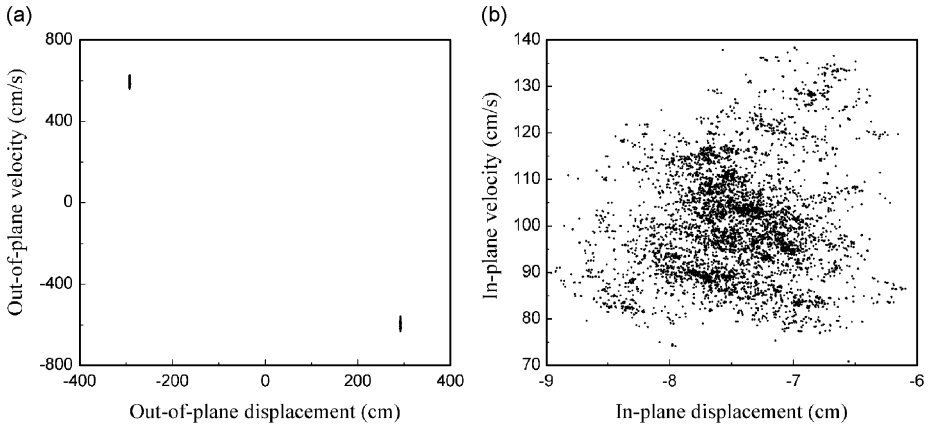

Fig. 12. Subharmonic response, $k = 2$. Poincaré map at the midpoint response with the ideal variable viscous damper. $U = 0.15$ m, $\Omega = 2\omega_1$.

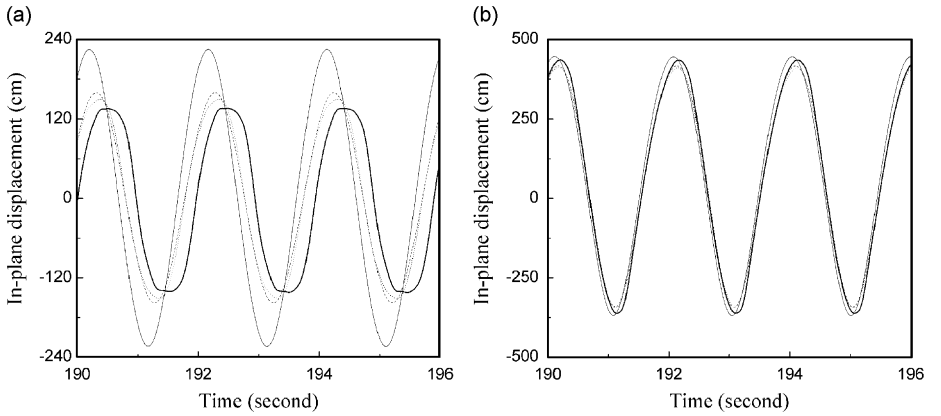

Fig. 13. Harmonic response, $k = 1$. In-plane displacement response at the midpoint. $\Omega = \omega_1$. (a) $U = 0.08$ m; (b) $U = 0.40$ m. Solid thin line: original cable. Dashed line: optimal viscous damper. Dotted line: MR damper using SA-1. Solid thick line: MR damper using SA-2.

In order to investigate the chaotic behaviour of the MR damper with the SA-2 control rule, the Poincaré map has shown in Fig. 11 when U is 0.15 m. It can be seen that the chaotic behaviour of the subharmonic out-of-plane component is moderate, whereas the harmonic in-plane vibration is completely chaotic. The Poincaré map of the variable viscous damper is shown in Figs. 12. The out-of-plane component is less chaotic, whereas the strong chaotic behaviour of the in-plane component occurs. Therefore, it is obvious that the chaotic phenomenon of the cable is mainly caused by the nonlinear semi-active control strategies.

5.2. Harmonic response, $\Omega \approx \omega_1$

At first, the chord elongation amplitude U is set to 0.08 m. The in-plane displacement time history at the midpoint is shown in Fig. 13(a). The peak value of the in-plane component $w_{\max}$ of the original cable is 225.3 cm. After the viscous damper and the MR damper are installed, the dynamic response is mitigated effectively, and $w_{\max}$ is reduced to about 159.8, 151.5 and 138.0 cm, respectively. In other words, dampers can provide about 29%, 33% and 39% reduction compared with the original cable, respectively. So the MR damper with the SA-2 rule is better than the optimal viscous damper. For the original cable and for the cable with viscous damper, the out-of-plane component will disappear eventually. By contrast, the MR dampers are

not able to eliminate the out-of-plane component completely. The reason is that although these two MR dampers are installed symmetrically at the same node of the cable, the displacements and hence the control signals for each MR damper are different because the motion of the cable is three-dimensional (see Eq. (17)). Therefore, the out-of-plane component of the resultant force provided by the MR dampers does always exist, which leads to the nonzero out-of-plane vibration.

Next, the amplitude U is increased to 0.40 m. Fig. 13(b) shows the in-plane response of the cable. The peak value of the original cable, of the cable with viscous dampers and of the cable with MR dampers using the different control rules are 446.3, 416.8, 411.6 and 435.8 cm, respectively, and in the best situation only about 7.8% reduction can be obtained by the damper compared with the original cable. The out-of-plane vibration of the cable without dampers and with viscous dampers will fade away after enough time. Once again, however small it is, there is an out-of-plane response of the cable supplied with the MR damper.

5.3. Superharmonic response, $\Omega \approx 2\omega_1/3$

At first, the amplitude U is set to 0.08 m. The numerical results show that only the in-plane vibration exists for both the undamped and the viscous-damped cable, so only the in-plane responses are shown in Fig. 14(a). For the undamped cable, the cable with viscous dampers, the cable with MR dampers using the SA-1 and SA-2 rules, the peak values of in-plane vibration are 23.0, 22.2, 22.2 and 22.8 cm, respectively. Therefore, neither the viscous damper nor the MR damper essentially has any capability to suppress the vibrations of the cable. As mentioned above, a small out-of-plane vibration component of the cable with MR dampers still exists.

Next, the amplitude U is increased to 0.40 m. Again, the superharmonic response is in-plane, as shown in Fig. 14(b). It can be seen that on the whole the viscous damper and the MR damper with the various control rules have little effect on the attenuation of the dynamic response of the cable.

Then the amplitude U is increased to 0.55 m. It is interesting to find that only in-plane vibration exists for the original cable and the MR dampers with the SA-2 rule, while the cable with the viscous dampers and the MR dampers with the SA-1 rule has a stable in-plane and out-of-plane coupled oscillation, as shown in Fig. 15. It can be seen that the maximum out-of-plane components for the latter two are almost the same, which is about 347.2 cm. The in-plane vibration is effectively mitigated by using dampers, and the peak-to-peak value is reduced from 642.2 cm for the original cable to 312.1 cm (viscous dampers), 306.5 cm (MR dampers with the SA-1 rule) and 397.3 cm (MR dampers with the SA-2 rule), respectively. Then, on the whole, the best control effect can be obtained using the MR dampers with the SA-2 rule. It is also clear in this case that the control concept based on energy dissipation has the maximum vibration reduction effect for the in-plane oscillation, which is achieved at a cost of a stable large-amplitude out-of-plane component.

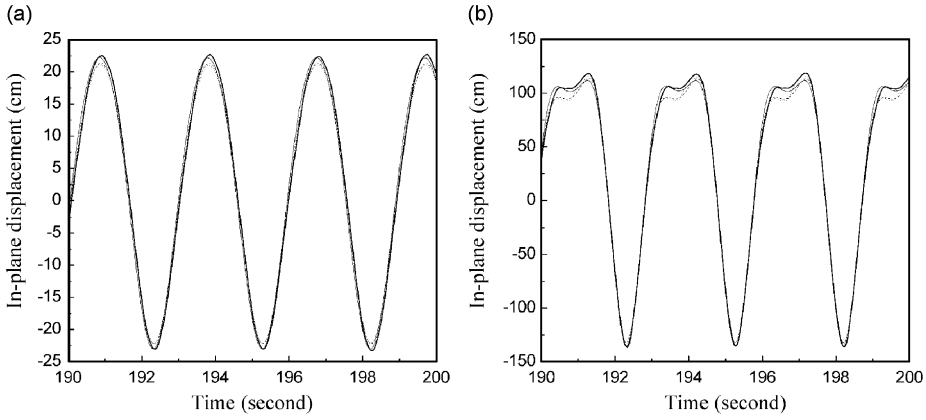

Fig. 14. Superharmonic response, $k = \frac{2}{3}$. In-plane displacement response at the midpoint. $\Omega = 2\omega_1/3$. (a) $U = 0.08$ m; (b) $U = 0.40$ m. Solid thin line: original cable. Dashed line: optimal viscous damper. Dotted line: MR damper using SA-1. Solid thick line: MR damper using SA-2.

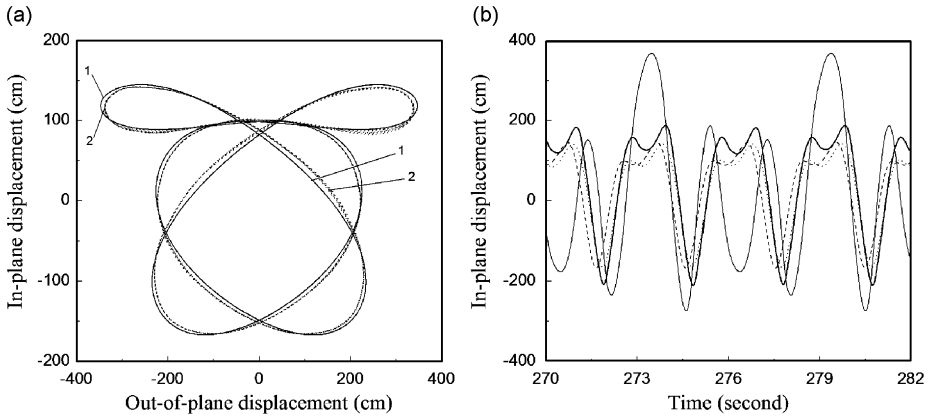

Fig. 15. Superharmonic response, $k=\frac{2}{3}$. $U=0.55\,\mathrm{m}$, $\Omega=2\omega_1/3$. (a) Trajectories at the midpoint. 1: optimal viscous damper. 2: MR damper using SA-1. (b) In-plane displacement response at the midpoint. Solid thin line: original cable. Dashed line: optimal viscous damper. Dotted line: MR damper using SA-1. Solid thick line: MR damper using SA-2.

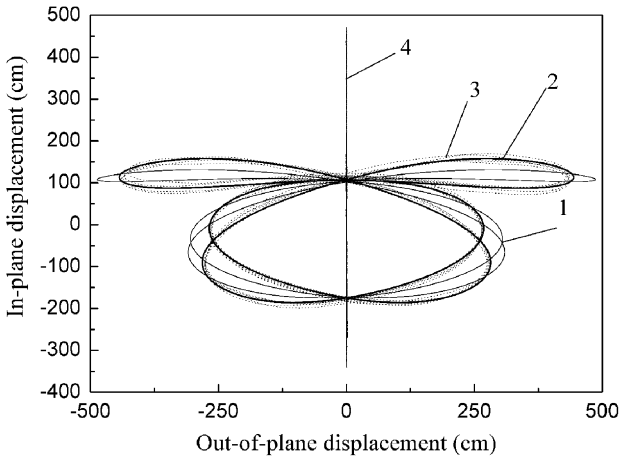

Fig. 16. Superharmonic response, $k=\frac{2}{3}$. Trajectories at the midpoint. $U=0.65\,\mathrm{m}$, $\Omega=2\omega_1/3$. 1: original cable. 2: optimal viscous damper. 3: MR damper using SA-1. 4: MR damper using SA-2.

Finally, the amplitude U is further increased to 0.65 m. In this case, the original cable is attracted to a motion with a stable out-of-plane component. Fig. 16 shows the trajectories at the midpoint of the cable. It can be seen that both the viscous damper and the MR damper can suppress the out-of-plane vibration of the cable somewhat. For the undamped cable the peak value of the out-of-plane component $v_{\max}$ is 486.8 cm, and that of the in-plane vibration $w_{\max}$ is 174.8 cm. For the cable with the viscous dampers and with the MR dampers using the SA-1 rule, $v_{\max}$ is reduced to 444.0 and 440.6 cm, and $w_{\max}$ is increased to 185.9 and 199.0 cm, respectively. Hence, both viscous damper and MR damper with the SA-1 rule have little effect on the attenuation of the vibration of the cable. When adopting the SA-2 control rule, the out-of-plane vibration is significantly suppressed, and $v_{\max}$ is less than 2.0 cm, while $w_{\max}$ increases as evidently as to 470.3 cm. Therefore, on the whole the control rule based on the balance logic principle is more effective than the control algorithm whose purpose is to dissipate the maximum amount of input energy.

Substituting the given data in the simplified Eq. (35), and U, is set to 0.55 and 0.65 m, respectively, it can be found that in both cases the out-of-plane vibration of the cable decays for the original cable and the cable with the passive or variable viscous dampers. However, when the in-plane and out-of-plane components interaction terms are considered, that is, Eq. (33) is used, it can be seen that when $U=0.55$ cm the periodic out-of-plane component of the cable exists only for the cable with the passive viscous dampers and when $U=0.65$ cm only

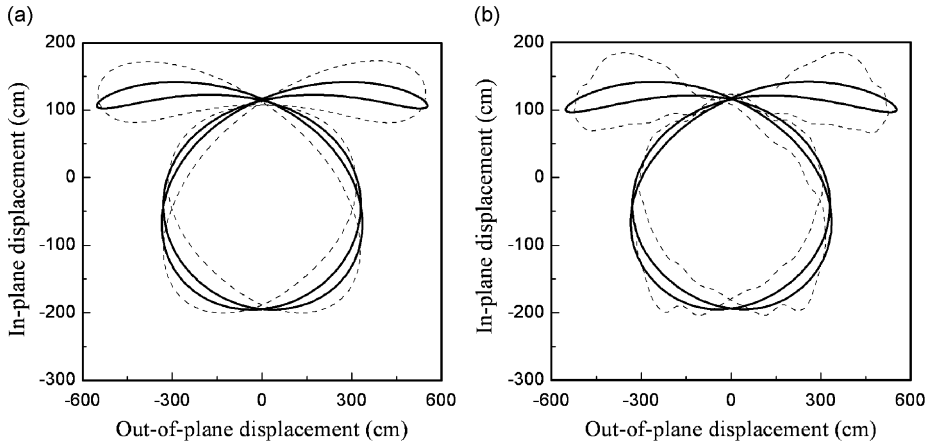

Fig. 17. Superharmonic response, $k=\frac{2}{3}$. Trajectories at the midpoint. $U=0.75\,\mathrm{m}$, $\Omega=2\omega_1/3$. (a) Solutions of simplified equation (33). (b) Solutions of FDM equations (21) and (22). Solid line: original cable. Dashed line: cable with ideal variable viscous dampers.

the cable with the variable viscous dampers is two-dimensional oscillation. Therefore, it can be concluded that the out-of-plane response of the original cable with $\Omega\approx 2\omega_1/3$ is mainly caused by two factors: one is that the amplitude of harmonic support motion exceeds a certain threshold, the other is the interaction between the in-plane and out-of-plane components, which is neglected in Eq. (35). Then, in order to reduce the out-of-plane component of the cable for $\Omega\approx 2\omega_1/3$ with larger support motion amplitude, it is important to suppress the in-plane and out-of-plane coupled vibration of the cable. Comparing the solutions obtained by Eq. (33) for the cable with variable dampers and that with passive dampers, it is obvious that mitigating the elastic force acting on the cable can effectively reduce the coupled motion while improperly improving the damping of the cable may augment the interaction in some cases.

Moreover, when $\Omega\approx 2\omega_1/3$ and $U=0.75\,\mathrm{m}$, the solutions of Eq. (33) for the cable with and without variable viscous dampers illustrate that both vibration is three-dimensional oscillation, and the trajectories at the midpoint are shown in Fig. 17, which also can be obtained by the rather complicated FDM Eqs. (21) and (22). The difference of solutions between these two models is mainly caused by the ignorance of higher modes in the simplified model. From Fig. 17 it can be deduced that the MR damper with the SA-2 rule has no vibration reduction effect on the out-of-pane component caused by superharmonic response when $\Omega\approx 2\omega_1/3$ and $U=0.75\,\mathrm{m}$. Therefore, the satisfactory control effect of out-of-plane vibration by the MR damper with the SA-2 rule can be achieved only when the support motion amplitude falls in a certain range, which is similar to the subharmonic response when $\Omega\approx 2\omega_1$. To some extent, the control effect provided by the MR damper with the SA-2 rule on the out-of-plane component of the cable under the support motion with $U=0.65$ and $0.75\,\mathrm{m}$ when $\Omega\approx 2\omega_1/3$ corresponds to that with $U=0.08$ and $0.15\,\mathrm{m}$ when $\Omega\approx 2\omega_1$, respectively.

Using the simplified equations. (33) and (35), it can be observed that there are two main differences for the trigger mechanism of out-of-plane vibration of cable without dampers when the support motion frequency is about $2\omega_1$ and $2\omega_1/3$. One is that for $\Omega\approx 2\omega_1$, small support motion amplitude can result in out-of-plane motion, while for $\Omega\approx 2\omega_1/3$ only excitation amplitude exceeds a large threshold the out-of-plane motion is possible. The other is that for $\Omega\approx 2\omega_1$ the large out-of-plane component is mainly caused by Mathieu-type parametric oscillation while for $\Omega\approx 2\omega_1/3$ the out-of-plane component is mainly induced by the in-plane and out-of-plane components interaction.

5.4. Superharmonic response, $\Omega\approx\omega_1/2$

At first, the amplitude U is set to $0.08\,\mathrm{m}$. Numerical results show that only the in-plane stable superharmonic vibrations of the undamped cable and the cable with viscous dampers exist, so only the in-plane response is shown in Fig. 18. The peak values of in-plane vibrations for the original cable, for the cable with viscous dampers and with MR dampers using the SA-1 and SA-2 rules are about 60.1, 30.6, 30.8 and

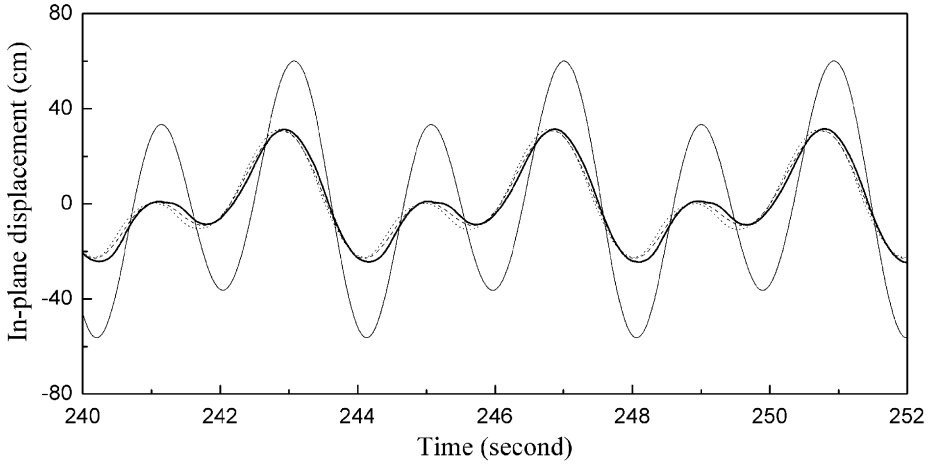

Fig. 18. Superharmonic response, $k=\frac{1}{2}$. In-plane displacement response at the midpoint. $U=0.08\,\mathrm{m}$, $\Omega=\omega_1/2$. Solid thin line: original cable. Dashed line: optimal viscous damper. Dotted line: MR damper using SA-1. Solid thick line: MR damper using SA-2.

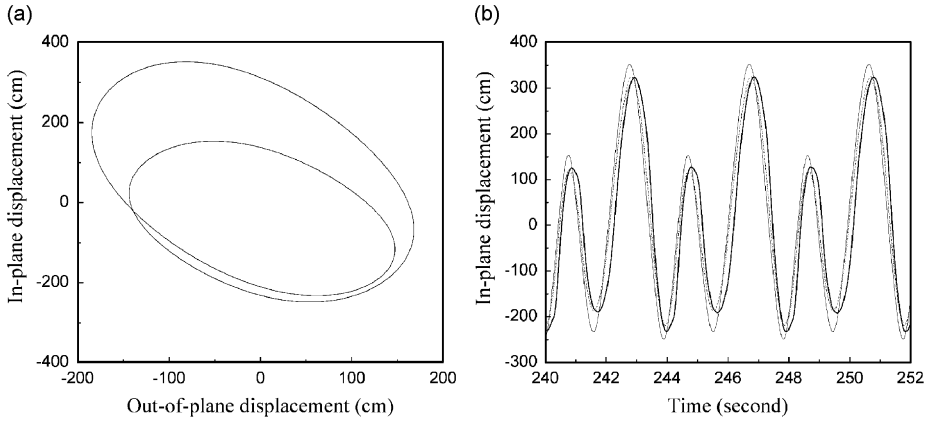

Fig. 19. Superharmonic response, $k=\frac{1}{2}$. $U=0.40\,\mathrm{m}$, $\Omega=\omega_1/2$. (a) Trajectory at the midpoint of the original cable. (b) In-plane displacement response at the midpoint. Solid thin line: original cable. Dashed line: optimal viscous damper. Dotted line: MR damper using SA-1. Solid thick line: MR damper using SA-2.

31.6 cm, respectively. Therefore, both the viscous damper and the MR damper have an effect in mitigating the dynamic response. Moreover, the vibration reduction effect provided by the viscous damper and the MR damper is comparable.

Next, U is increased to 0.40 m. Fig. 19(a) shows the trajectory at the midpoint of the original cable. The peak value of the out-of-plane component $v_{\max}$ is 184.4 cm, and that of the in-plane component is $w_{\max}=352.0\,\mathrm{cm}$. After the viscous dampers are equipped, the out-of-plane vibration is eliminated. For the MR damper, the nonzero out-of-plane component remains for the above-mentioned reason. However, the peak value of the out-of-plane component is less than 6.0 cm. Therefore, the influence of the out-of-plane vibration at the midpoint of the cable can be neglected compared with the in-plane component. Fig. 19(b) shows the in-plane response of the cable. It can be seen that the viscous damper and the MR damper using the different control algorithms provide comparable results. $w_{\max}$ for the viscous damper and for the MR damper with the different control rules are about 325.3, 313.9 and 327.9 cm, respectively. Therefore, as far as the in-plane vibration reduction is concerned, neither the viscous damper nor the MR damper has any significant effect on the reduction of the superharmonic response. Using the simplified model (33), it also can be found that the out-of-plane component of the cable with the passive or variable viscous dampers disappear eventually even for $U=0.75\,\mathrm{m}$.

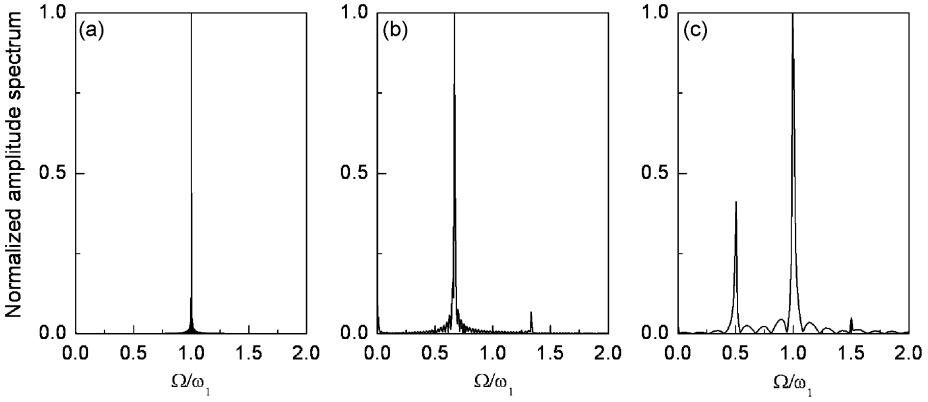

Fig. 20. Normalized amplitude spectrum of in-plane vibration at the midpoint of the original cable. $U = 0.08$ m. (a) $\Omega \approx \omega_1$; (b) $\Omega \approx 2\omega_1/3$; (c) $\Omega \approx \omega_1/2$.

When the support motion frequency is about ω_1, $2\omega_1/3$ and $\omega_1/2$, Fig. 20 displays the normalized amplitude spectrum of the in-plane component at the midpoint of the original cable with $U = 0.08$ m. It can be observed that when $\Omega \approx \omega_1$ and $\omega_1/2$ most vibration energy concentrate at ω_1, that is, the in-plane vibration is dominated by the first in-plane symmetric mode, while when $\Omega \approx 2\omega_1/3$ most vibration energy focus at $2\omega_1/3$. This may be the reason as to why the control effect provided by the damper is insignificant for $\Omega \approx 2\omega_1/3$ but satisfactory for $\Omega \approx \omega_1$ and $\omega_1/2$ with smaller support motion amplitude, as shown in Figs. 13(a), 14(a) and 18.

By the way, it should be noted that the simplified model (33), in which the in-plane and out-of-plane oscillation interaction is taken into consideration, covers some essential dynamic properties of the cable with and without dampers.

6. Conclusions

The control of the sub- and superharmonic responses of an inclined shallow cable with MR dampers under harmonic support motion is investigated. Semi-active control strategies based on the modulated homogeneous friction (SA-1) rule and the balance logic (SA-2) rule are proposed. The main goal of the former is to dissipate as much as possible of the input energy, while that of the latter is to reduce or balance the elastic force acting on the cable. Because only the displacement and the velocity responses of the MR dampers are required, the proposed control rules are easy to implement.

In particular the four cases, where the harmonic frequency of the support point motion Ω approaches $2\omega_1$, ω_1, $2\omega_1/3$, and $\omega_1/2$, are analysed. The vibration reduction ability with MR dampers is verified by comparison with the optimal viscous damper tuned to the first in-plane eigenmode of the cable. The numerical results show that the MR damper with the SA-1 rule and the optimal viscous damper perform similarly to suppress the vibration of the cable under periodic chord elongation, and, in some cases, the SA-2 rule is more favourable than the SA-1 rule in mitigating the out-of-plane vibration of the cable. The optimal viscous damper and the MR damper with the proposed control rules can effectively mitigate the out-of-plane vibration of the cable for the subharmonic case $\Omega \approx 2\omega_1$ with a rather small excitation amplitude and the superharmonic case $\Omega \approx \omega_1/2$ with a larger excitation amplitude. Especially, in the subharmonic case $\Omega \approx 2\omega_1$ with a small excitation amplitude, and in the superharmonic case $\Omega \approx 2\omega_1/3$ with a rather large excitation amplitude falling in a certain range, the SA-2 control rule is much better than the SA-1 rule and the optimal viscous damper in suppressing the out-of-plane vibrations. Moreover, when $\Omega \approx 2\omega_1/3$ the control strategy should be selected carefully. Contrary to the common viewpoint, when the amplitude of the harmonic support motion falls in a certain range, the vibration mode of the cable should be changed from the original zero out-of-plane vibration to the stable periodic large amplitude out-of-plane response by using the optimal passive viscous dampers or the MR dampers with the control algorithm based on energy dissipation criterion. In addition, the in-plane component only during the harmonic response $\Omega \approx \omega_1$ and the superharmonic response $\Omega \approx \omega_1/2$ can be effectively reduced by the MR damper and the viscous damper, if the excitation amplitude is sufficiently small.

It is also observed that the vibrations of the cable become chaotic when the cable is supplied with the MR damper using the proposed nonlinear control algorithms.

Acknowledgements

The first writer gratefully acknowledges for the financial support from the Chenguang Project of Wuhan City under Grant 20025001031, and a visiting appointment at the Aalborg University, Denmark. The financial support from Major International Joint Research Program under Grant 50520130296 is also appreciated.

References

[1] S.C. Watson, D. Stafford, Cables in trouble, *Civil Engineering, ASCE* 58 (1988) 38–41.
[2] N.J. Gimsing, *Cable Supported Bridges: Concept and Design*, second ed., Wiley, 1997.
[3] I. Kovacs, Zur Frage der Seilschwingungen und der Seildampfung, *Die Bautechnik* 59 (1981) 325–332 (in German).
[4] B.M. Pacheo, Y. Fujino, A. Sulekh, Estimation curve for modal damping in stay cables with viscous damper, *Journal of Structural Engineering, ASCE* 119 (1993) 1961–1979.
[5] Z. Yu, Y.L. Xu, Mitigation of three-dimensional vibration of inclined sag cable using discrete oil dampers. I. Formulation, *Journal of Sound and Vibration* 214 (1998) 659–673.
[6] S. Krenk, Vibrations of a taut cable with an external damper, *Journal of Applied Mechanics* 67 (2000) 772–776.
[7] S. Krenk, S.R.K. Nielsen, Vibrations of a shallow cable with a viscous damper, *Proceeding of the Royal Society of London Series A* 458 (2002) 339–357.
[8] J.A. Main, N.P. Jones, Free vibrations of taut cable with attached damper. I: Linear viscous damper, *Journal of Engineering Mechanics, ASCE* 128 (2002) 1062–1071.
[9] T. Susupow, Y. Fujino, Active control of multimodal cable vibrations by axial support motion, *Journal of Engineering Mechanics, ASCE* 121 (1995) 964–972.
[10] Y. Achkire, Active Tendon Control of Cable-stayed Bridges, PhD Thesis, ULB, Belgium, 1997.
[11] A. Preumont, F. Bossens, Active tendon control of cable-stayed bridges: a large-scale demonstration, *Earthquake Engineering and Structural Dynamics* 30 (2001) 961–979.
[12] E.A. Johnson, R.E. Christenson, B.F. Spencer Jr., Semiactive damping of cables with sag, *Computer Aided Civil and Infrastructure Engineering* 18 (2003) 132–146.
[13] Y.Q. Ni, Y. Chen, J.M. Ko, D.Q. Cao, Neuro-control of cable vibration using semi-active magneto-rheological dampers, *Engineering Structures* 24 (2002) 295–307.
[14] Q. Zhou, S.R.K. Nielsen, W.L. Qu, Semi-active control of three-dimensional vibration of inclined sag cable with MR dampers, *Journal of Sound and Vibration* 296 (2006) 1–22.
[15] R.E. Christenson, B.F. Spencer Jr., E.A. Johnson, Experimental verification of smart cable damping, *Journal of Engineering Mechanics, ASCE* 132 (2006) 268–278.
[16] Y.Q. Ni, J.M. Ko, Z.Q. Chen, B.F. Spencer Jr., Lessons learned from application of semiactive MR dampers to bridge cables for wind-rain-induced vibration control, *China–Japan Workshop on Vibration Control and Health Monitoring of Structures and Third Chinese Symposium on Structural Vibration Control*, Shanghai, China, 2002.
[17] Z.Q. Chen, X.Y. Wang, Y.Q. Ni, J.M. Ko, Field measurements on wind-rain-induced vibration of bridge cables with and without MR dampers. *The Third World Conference on Structural Control*, Como, Italy, 2002.
[18] N.C. Perkins, Modal interactions in the nonlinear response of elastic cables under parametric/external excitation, *International Journal of Nonlinear Mechanics* 27 (1992) 233–250.
[19] F. Benedettini, G. Rega, R. Alaggio, Nonlinear oscillations of a four-degree-of-freedom model of a suspension cable under multiple internal resonance conditions, *Journal of Sound and Vibration* 182 (1995) 775–798.
[20] G. Rega, R. Alaggio, F. Benedettini, Experimental investigation of the nonlinear response of a hanging cable. Part I: Local analysis, *Nonlinear Dynamics* 14 (1997) 89–117.
[21] F. Benedettini, G. Rega, Experimental investigation of the nonlinear response of a hanging cable. Part II: Global analysis, *Nonlinear Dynamics* 14 (1997) 119–138.
[22] S.R.K. Nielsen, P.H. Kirkegaard, Super and combinatorial harmonic response of flexible elastic cables with small sag, *Journal of Sound and Vibration* 251 (2002) 79–102.
[23] J.W. Larsen, S.R.K. Nielsen, Nonlinear stochastic response of a shallow cable, *International Journal of Nonlinear Mechanics* 41 (2006) 327–344.
[24] A. Pinto da Costa, J.A.C. Martins, F. Branco, J.L. Lilien, Oscillations of bridge stay cables induced by periodic motions of deck and/or tower, *Journal of Engineering Mechanics, ASCE* 122 (1996) 613–622.
[25] Q. Zhou, W.L. Qu, Two mechanical models for magnetorheological damper and corresponding test verification, *Earthquake Engineering and Engineering Vibration* 22 (2002) 144–150 (in Chinese).
[26] B.F. Spencer Jr., S.J. Dyke, M.K. Sain, J.D. Carlson, Phenomenological model for magnetorheological damper, *Journal of Engineering Mechanics, ASCE* 123 (1997) 230–238.

[27] H. Tabatabai, A.B. Mehrabi, Design of mechanical viscous dampers for stay cables, *Journal of Bridge Engineering, ASCE* 5 (2000) 114–123.
[28] H.M. Irvine, *Cable Structures*, MIT Press, Cambridge, MA, 1981.
[29] M. El-Attar, A. Ghobarah, T.S. Aziz, Non-linear cable response to multiple support periodic excitation, *Engineering Structures* 22 (2000) 1301–1312.
[30] K.J. Bathe, *Finite Element Procedures In Engineering Analysis*, Prentice-Hall, Englewood Cliffs, NJ, 1982.
[31] J.A. Inaudi, Modulated homogeneous friction: a semi-active damping strategy, *Earthquake Engineering and Structural Dynamics* 26 (1997) 361–376.
[32] C.W. Stammers, T. Sireteanu, Vibration control of machines by use of semi-active dry friction damping, *Journal of Sound and Vibration* 209 (1998) 671–684.
[33] T.T. Soong, *Active Structure Control: Theory and Practice*, Longman Scientific & Technical, New York, 1990.
[34] E.A. Johnson, G.A. Baker, B.F. Spencer Jr., Y. Fujino, Semiactive damping of stay cables, *Journal of Engineering Mechanics, ASCE* 133 (2007) 1–11.
[35] Y.L. Xu, Z. Yu, Mitigation of three-dimensional vibration of inclined sag cable using discrete oil dampers. II: Application, *Journal of Sound and Vibration* 214 (1998) 675–693.